



Human
Biomics
Lab



Kathryn Weber
Juliana Delben
Timothy G. Bromage
Simone Duarte

Comparison of SEM and VPSEM imaging techniques with respect to *Streptococcus mutans* biofilm topography

Comparison of SEM and VPSEM imaging techniques with respect to *Streptococcus mutans* biofilm topography

Kathryn Weber¹, Juliana Delben¹, Timothy G. Bromage² & Simone Duarte¹

¹Basic Science and Craniofacial Biology, New York University College of Dentistry, New York, NY, USA; and ²Department of Biomaterials and Biomimetics, New York University College of Dentistry, New York, NY, USA

Correspondence: Simone Duarte, Department of Basic Science and Craniofacial Biology, NYU College of Dentistry, Room 921c Schwartz Hall, 345 E. 24th Street, New York, NY 10010, USA.
Tel.: +1 212 9989572;
fax: +1 212 9954087;
e-mail: sd84@nyu.edu

Received 15 October 2013; revised 31 October 2013; accepted 13 November 2013.
Final version published online 2 December 2013.

DOI: 10.1111/1574-6968.12334

Editor: David Clarke

Keywords

biofilm; extracellular polymeric substance; *Streptococcus mutans*; SEM; VPSEM.

Introduction

Streptococcus mutans is a facultatively anaerobic, Gram-positive bacterium that is a major contributor to dental caries and in some cases a progenitor to endocarditis (Loeche, 1986). The bacterial cells adhere to tooth surfaces using the extracellular polymeric substance (EPS), specifically the molecule glucan in *S. mutans* biofilms (Rahim & Thurairajah, 2011). Production of the glucan and the EPS increases when in the presence of sucrose and glucosyl-transferase activity, but with limited nitrogen, potassium, and phosphate in the medium (Fulcher *et al.*, 2001; Donlan & Costerton, 2002; Rahim & Thurairajah, 2011). The EPS is required during the initial attachment of bacterial cells to the tooth surface, as the polysaccharides form hydrophobic and ionic interactions between the host receptors and the bacterial adhesions (Marsh, 2004). The microorganisms switch from a planktonic phenotype in fluid to a sessile phenotype on the tooth surface, triggering the formation of the polysaccharide-rich EPS and decreasing the mitotic activity of the bacterial cell (Jakubovics & Kolenbrander,

Abstract

The study compared images of mature *Streptococcus mutans* biofilms captured at increasing magnification to determine which microscopy method is most acceptable for imaging the biofilm topography and the extracellular polymeric substance (EPS). *In vitro* *S. mutans* biofilms were imaged using (1) scanning electron microscopy (SEM), which requires a dehydration process; (2) SEM and ruthenium red (SEM-RR), which has been shown to support the EPS of biofilms during the SEM dehydration; and (3) variable pressure scanning electron microscopy (VPSEM), which does not require the intensive dehydration process of SEM. The dehydration process and high chamber vacuum of both SEM techniques devastated the biofilm EPS, removed supporting structures, and caused cracking on the biofilm surface. The VPSEM offered the most comprehensive representation of the *S. mutans* biofilm morphology. VPSEM provides similar contrast and focus as the SEM, but the procedure is far less time-consuming, and the use of hazardous chemicals associated with SEM dehydration protocol is avoided with the VPSEM. The inaccurate representations of the biofilm EPS in SEM experimentation is a possible source of inaccurate data and impediments in the study of *S. mutans* biofilms.

2010). The EPS provides a physical barrier that inhibits attachment to macrophages and phagocytes, while the reduced metabolic activity precludes the use of antibiotics that act on bacteria during growth periods (Schwarzmann & Boring, 1971; Whitnack *et al.*, 1981). The EPS can also contribute to resistance to antibiotics through the formation of bacterial ‘towers’ surrounded by polysaccharide to reduce physical contact between the antimicrobials and viable cells (Hoyle & Costerton, 1991; Xiao *et al.*, 2012). Another function of the EPS is to ensure that the biofilm remains hydrated, as the polymeric substance retains water and reinforces water channels to prevent desiccation of the structure and to deliver nutrients to the aggregate (Flemming *et al.*, 2007). The EPS contributes to the dynamic arrangement of the biofilm, which allows the colony to withstand turbulent fluid forces within the oral cavity (Donlan & Costerton, 2002). The EPS is also important in the accumulation of immigrant bacterial cells into the diverse biofilm composition, leading to greater genetic exchange and diversity within the aggregate (Flemming *et al.*, 2007; Lemos *et al.*, 2013).

Considering that EPS is such an integral component of the biofilm and it is a crucial target for biofilm disruption experimentation, there is a need to evaluate different microscopy protocols to provide the most accurate representation of *S. mutans* biofilm structure and morphology. Techniques that preserve the biofilm matrix are highly desired and frequently studied, however, these methods are not all encompassing with respect to species and experimental setups. Scanning electron microscopy (SEM) allows for the visualization of sample topography and generates a three-dimensional appearance of the substance (Hannig *et al.*, 2010). However, high vacuum pressure is needed to evaluate the samples, and the biofilm must be fixed, dehydrated, and sputter-coated with a conductive metal such as gold to ensure electrical conductivity (Muscariello *et al.*, 2005; Hannig *et al.*, 2010). The result is an artifact of the original sample due to the intensive dehydration protocol (Ishii *et al.*, 2004), which leads to loss of biofilm structures, specifically of the EPS (Priester *et al.*, 2007). Previous research on biofilms attributes the use of cationic ruthenium red (RR) during the SEM fixation process to the preservation of sugar compounds of the EPS in biofilm samples, the identification of extracellular fibers, and the prevention of shrinking the sample (Figueroa & Silverstein, 1989; Fassel & Edmiston, 1999; Fulcher *et al.*, 2001; Erlandsen *et al.*, 2004). RR is assumed to stabilize the biofilm EPS through nonspecific electrostatic or ionic attraction to the matrix (Fassel & Edmiston, 1999). Variable pressure scanning electron microscopy (VPSEM) is another available option to image biofilms. Unlike the high vacuum pressure and dry conditions of the SEM sample chamber, the VPSEM samples can be imaged at diverse pressure and vacuum settings at an increased humidity (Priester *et al.*, 2007). This study compared these three techniques (SEM, SEM with RR, and VPSEM) to determine which imaging protocol is most effective for observing *S. mutans* biofilms morphology with respect to topography and EPS preservation.

Materials and methods

Biofilm preparation

Streptococcus mutans UA159 biofilms were prepared as described elsewhere (Duarte *et al.*, 2006). Saliva-coated hydroxyapatite disks were used as substrate, and the biofilm was formed in tryptone soy broth with yeast extract (TSB + YE) media with 1% sucrose that had been inoculated with *S. mutans*. The media containing 1% sucrose solution in TSB + YE was changed every 24 h, for 5 days. Two hydroxyapatite disk samples were imaged for each microscopy technique (SEM, SEM with RR, and VPSEM) with four replicate studies performed in each condition.

SEM protocol (SEM group)

Samples were transferred to wells containing 1 mL of 2.5% glutaraldehyde solution for 2 h. Then, the samples were rinsed three times in phosphate-buffered saline (PBS) solution. The disks were exposed to 1% osmium tetroxide (OsO₄) for 1 h and then were dehydrated with increasing ethanol percentages (35%, 50%, 75%, 2 × 90%, and 2 × 100%) for 30 min in each solution. Samples were immersed in hexamethyldisilazane for 1.5 h and then placed in a desiccator for 12 h. Each disk was gold sputter-coated and mounted on a glass slide (Basso *et al.*, 2011). Images were captured using the SEM Hitachi S-3500N (Hitachi High Technologies America, Inc., Pleasanton, CA).

RR SEM protocol (SEM-RR group)

Samples were transferred to wells containing 1 mL of 2.5% glutaraldehyde solution and 0.5 mg RR for 2 h. Next, the disks were rinsed 5 min each in 1 mL PBS with 0.5 mg RR. This step was performed three times in new wells for each washing. Then, the samples were transferred to wells containing 1 mL of 1% OsO₄ and 0.5 mg RR for 1 h. The ethanol dehydrations, hexamethyldisilazane dehydration, desiccation, and gold sputter coating were kept in congruence with the SEM protocol above. Images were captured using the SEM Hitachi S-3500N (Hitachi High Technologies America, Inc.).

VPSEM protocol (VPSEM group)

Samples were transferred directly to the VPSEM [Zeiss EVO 50 (Carl Zeiss Microscopy, LLC, Thornwood, NY) chamber and imaged at 100 Pa, selected after previous experiments (data not shown) to analyze the best pressure to preserve the EPS.

All SEM, SEM-RR, and VPSEM images were captured at a working distance of 8.5 mm and field widths of *c.* 1 mm, 100 μm, 40 μm, and 20 μm.

Results and discussion

Visual comparison of the SEM, SEM-RR, and VPSEM images at each respective field width is shown in Figs 1, 2, 3, and 4. There was no visual difference between the EPS present in the SEM and SEM-RR samples. The VPSEM better maintained the EPS than the SEM and SEM-RR samples. There was no visual difference between the SEM and SEM-RR with respect to EPS prevalence. SEM groups (Fig. 1a and b) exhibited cracking in the biofilm topography, whereas the VPSEM image (Fig. 1c) did not demonstrate the cracking phenomenon.

Fig. 1. *Streptococcus mutans* biofilms imaged using SEM by Hitachi (a), SEM with RR (b), and the VPSEM (variable pressure SEM) by Zeiss (c) techniques. Images (a, b, and c) were compared at working distance of 8.5 mm and field width of c. 1 mm.

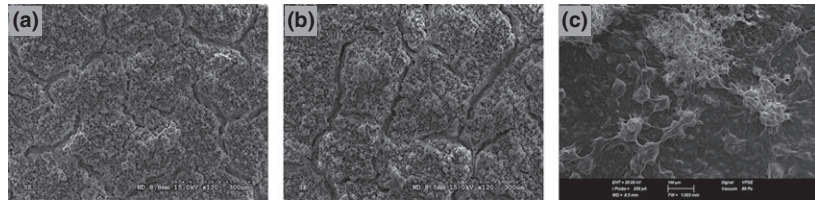


Fig. 2. *Streptococcus mutans* biofilms imaged using SEM by Hitachi (a), SEM with RR (b), and the VPSEM (variable pressure SEM) by Zeiss (c) techniques. Images (a, b, and c) were captured and compared at a working distance of 8.5 mm and a field width of c. 100 μm .

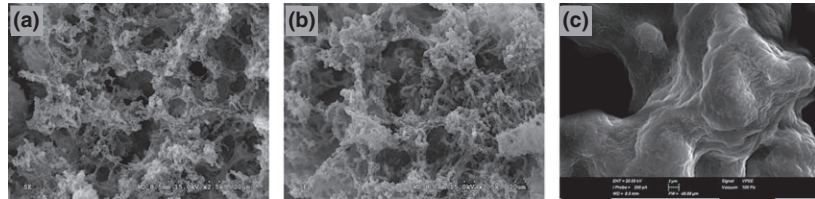


Fig. 3. *Streptococcus mutans* biofilms imaged using SEM by Hitachi (a), SEM with RR (b), and the VPSEM (variable pressure SEM) by Zeiss (c) techniques. Images (a, b, and c) were captured at a working distance of 8.5 mm and a field width of c. 40 μm .

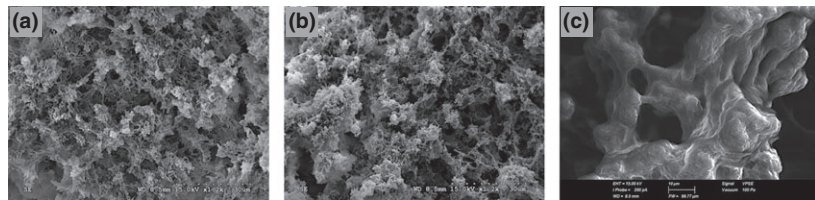
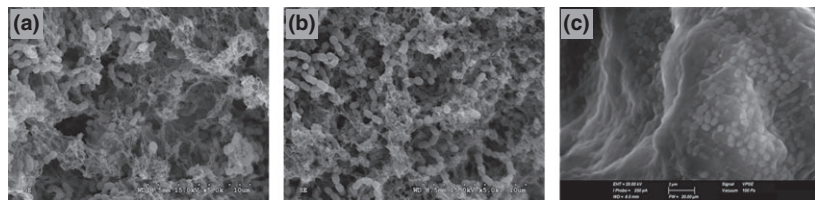


Fig. 4. *Streptococcus mutans* biofilms imaged using SEM by Hitachi (a), SEM with RR (b), and the VPSEM (variable pressure SEM) by Zeiss (c) techniques. Images (a, b, and c) were photographed and analyzed at a working distance of 8.5 mm and a field width of c. 20 μm .



Connective EPS structures between ‘bacterial towers’ were more common in the VPSEM samples (Fig. 2). Dark round spots within the biofilms, which we assume are topographical water channels, were also better defined when using the VPSEM microscope (Figs 1 and 3). All three techniques preserved the individual *S. mutans* cells, but the VPSEM maintained more structural components attributed to the EPS and the topographical morphology.

When comparing SEM, SEM-RR, and VPSEM imaging techniques, this study suggests that the VPSEM is the most accurate of these three methods to image the EPS matrix morphology of *S. mutans* biofilms with respect to topography. The SEM does not provide an accurate assessment of the biofilm morphology and topography because the EPS matrix is subject to destruction via the dehydration process and high pressure required for SEM. For this reason, both the SEM and SEM-RR dehydrations were compared to determine whether the RR better maintained the biofilm EPS. There was no discernible difference between the

amounts of EPS in either SEM group, indicating that RR did not effectively preserve the EPS of *S. mutans*. Our results were most likely not in congruence with previous experimentation that used RR to maintain the EPS because *S. mutans* biofilms were tested as opposed to *Enterococcus faecalis*, *Klebsiella pneumonia*, or staphylococcal species used in previous studies with SEM and RR (Fassel & Edmiston, 1999; Erlandsen *et al.*, 2004). Therefore, it is proposed that polysaccharide-rich EPS structure in *S. mutans* does not make it a viable candidate for RR staining prior to imaging by preventing the nonspecific electrostatic or ionic interactions between the RR and the EPS. On the contrary, the VPSEM protocol revealed a much greater amount of EPS when compared to both SEM protocols and is therefore the most viable method of studying *S. mutans* biofilm EPS matrix morphology tested in this experiment (Figs 1, 2, 3, and 4).

Biofilms are composed of c. 85% EPS and 15% bacterial cells, and in *S. mutans* biofilm, the EPS strongly

contributes to the antibiotic resistance, host evasion, hydration, maturation, adhesion, and structural support (Fulcher *et al.*, 2001; Rahim & Thurairajah, 2011; Xiao *et al.*, 2012). Although previous studies (Ishii *et al.*, 2004; Weimer *et al.*, 2006) have demonstrated the benefits of using VPSEM to visualize other biofilms under humid conditions as SEM protocol destroys the majority of the biofilm structure (Donlan & Costerton, 2002; Priester *et al.*, 2007), several studies analyze the matrix of *S. mutans* biofilm by SEM (da Cunha *et al.*, 2013; Fu *et al.*, 2013; Wang *et al.*, 2013). In addition, the biofilm matrix of *S. mutans* biofilm is commonly imaged by SEM during disruption experimentation, but our results indicated that VPSEM provided a more accurate image of the *S. mutans* biofilm morphology with respect to topography and EPS content. Based on our results, SEM is not an ideal method to evaluate disruption of the EPS, as the SEM protocol obliterates the polysaccharide matrix indicator in disruption experiments (Xue *et al.*, 2011). Therefore, previous disruption experimentation using SEM is called into question as the SEM protocol may produce misleading results.

The individual cells in the SEM did not appear to be altered by the dehydration process and may be more accessible for experimentation concerning cellular shape, death, and quantity. Because SEM is readily available and cost-effective, it is often the method used to image biofilms, but the VPSEM provides similar contrast and focus as the SEM, but the procedure is far less time-consuming and the use of hazardous chemicals associated with SEM dehydration protocol is avoided with the VPSEM (Staniewicz *et al.*, 2012). The inaccurate representation of the biofilm EPS in SEM experimentation is a possible source of inaccurate data and impediments in the study of *S. mutans* biofilms.

Other techniques are also available to image individual *S. mutans* cells and can achieve greater magnifications including scanning transmission electron microscopy (TEM), confocal microscopy, and atomic force microscopy (Priester *et al.*, 2007; Reese & Guggenheim, 2007; Xue *et al.*, 2011). According to Reese and Guggenheim, TEM can produce artifact-free images and provide clear ultrastructures in a multi-species biofilm. Although the updated TEM method is beneficial, the VPSEM allows for unaltered samples to be visualized immediately (without chemical alteration) and maintains the ultrastructure. Indeed, the challenge of imaging unprepared biofilm is not with the VPSEM, but with the coating unit required to deposit a conductive layer of metal or carbon on the surface for traditional SEM. It is the vacuum of the coating unit that dehydrates and deforms the biofilm. VPSEM eliminates the need for vacuum evaporation of a conductive coating, and thus, the pressures used in this study were sufficient to generate a useful signal, while not

being so high as to dehydrate the specimen. VPSEM and other forms of low-vacuum imaging in the SEM is becoming more common, and our study is a reminder to those acquiring such technologies that their work on materials such as biofilm can be performed without the need for high vacuum in either the coating unit or the SEM. Currently, the best method to examine the components of the biofilm is to incorporate multiple microscopy techniques to observe the 3-D structure, EPS content, morphology, topography, cellular components, spatial relationships, and environmental interaction (Alhede *et al.*, 2012).

This study is of high significance to the medical field as it contributes to the understanding of biofilm communities, addressing one of the most important contributors for the increased virulence, pathogenicity, and resistance of biofilms, the extracellular polysaccharide matrix. It will have a direct impact on the imaging techniques used to study biofilm morphology, mainly in relation to the extracellular matrix. The microscopy techniques analyzed are generic and thus applicable to biofilms associated with other microorganisms.

Acknowledgements

This work was supported by New York University College of Dentistry, Department of Basic Science and Craniofacial Biology. The authors are thankful for the technology support provided by Christopher Ferrante. There is no financial relationship related to the companies that manufactures the products discussed in this presentation.

References

- Alhede M, Qvortrup K, Liebrechts R, Hoiby N, Givskov M & Bjarnsholt T (2012) Combination of microscopic techniques reveals a comprehensive visual impression of biofilm structure and composition. *FEMS Immunol Med Microbiol* **65**: 335–342.
- Basso FG, Oliveira CF, Fontana A *et al.* (2011) *In vitro* effect of low-level laser therapy on typical oral microbial biofilms. *Braz Dent J* **22**: 502–510.
- da Cunha MG, Franchin M, Galvao LC, Bueno-Silva B, Ikegaki M, de Alencar SM & Rosalen PL (2013) Apolar bioactive fraction of *Melipona scutellaris* geopropolis on *Streptococcus mutans* biofilm. *Evid Based Complement Alternat Med* **2013**: 256287.
- Donlan RM & Costerton JW (2002) Biofilms: survival mechanisms of clinically relevant microorganisms. *Clin Microbiol Rev* **15**: 167–193.
- Duarte S, Gregoire S, Singh AP, Vorsa N, Schaich K, Bowen WH & Koo H (2006) Inhibitory effects of cranberry polyphenols on formation and acidogenicity of *Streptococcus mutans* biofilms. *FEMS Microbiol Lett* **257**: 50–56.

- Erlandsen SL, Kristich CJ, Dunny GM & Wells CL (2004) High-resolution visualization of the microbial glycocalyx with low-voltage scanning electron microscopy: dependence on cationic dyes. *J Histochem Cytochem* **52**: 1427–1435.
- Fassel TA & Edmiston CE Jr (1999) Ruthenium red and the bacterial glycocalyx. *Biotech Histochem* **74**: 194–212.
- Figuerola LA & Silverstein JA (1989) Ruthenium red adsorption method for measurement of extracellular polysaccharides in sludge flocs. *Biotechnol Bioeng* **33**: 941–947.
- Fleming HC, Neu TR & Wozniak DJ (2007) The EPS matrix: the “house of biofilm cells”. *J Bacteriol* **189**: 7945–7947.
- Fu D, Pei D, Huang C, Liu Y, Du X & Sun H (2013) Effect of desensitising paste containing 8% arginine and calcium carbonate on biofilm formation of *Streptococcus mutans in vitro*. *J Dent* **41**: 619–627.
- Fulcher TP, Dart JK, McLaughlin-Borlace L, Howes R, Matheson M & Cree I (2001) Demonstration of biofilm in infectious crystalline keratopathy using ruthenium red and electron microscopy. *Ophthalmology* **108**: 1088–1092.
- Hannig C, Follo M, Hellwig E & Al-Ahmad A (2010) Visualization of adherent micro-organisms using different techniques. *J Med Microbiol* **59**: 1–7.
- Hoyle BD & Costerton JW (1991) Bacterial resistance to antibiotics: the role of biofilms. *Prog Drug Res* **37**: 91–105.
- Ishii S, Koki J, Unno H & Hori K (2004) Two morphological types of cell appendages on a strongly adhesive bacterium, *Acinetobacter* sp. strain Tol 5. *Appl Environ Microbiol* **70**: 5026–5029.
- Jakubovics NS & Kolenbrander PE (2010) The road to ruin: the formation of disease-associated oral biofilms. *Oral Dis* **16**: 729–739.
- Lemos JA, Quivey RG Jr, Koo H & Abranches J (2013) *Streptococcus mutans*: a new Gram-positive paradigm? *Microbiology* **159**: 436–445.
- Loesche WJ (1986) Role of *Streptococcus mutans* in human dental decay. *Microbiol Rev* **50**: 353–380.
- Marsh PD (2004) Dental plaque as a microbial biofilm. *Caries Res* **38**: 204–211.
- Muscariello L, Rosso F, Marino G, Giordano A, Barbarisi M, Cafiero G & Barbarisi A (2005) A critical overview of ESEM applications in the biological field. *J Cell Physiol* **205**: 328–334.
- Priester JH, Horst AM, Van de Werfhorst LC, Saleta JL, Mertes LA & Holden PA (2007) Enhanced visualization of microbial biofilms by staining and environmental scanning electron microscopy. *J Microbiol Methods* **68**: 577–587.
- Rahim ZH & Thurairajah N (2011) Scanning electron microscopic study of *Piper betle* L. leaves extract effect against *Streptococcus mutans* ATCC 25175. *J Appl Oral Sci* **19**: 137–146.
- Reese S & Guggenheim B (2007) A novel TEM contrasting technique for extracellular polysaccharides in *in vitro* biofilms. *Microsc Res Tech* **70**: 816–822.
- Schwarzmann S & Boring JR (1971) Antiphagocytic effect of slime from a mucoid strain of *Pseudomonas aeruginosa*. *Infect Immun* **3**: 762–767.
- Staniewicz L, Donald AM, Stokes DJ *et al.* (2012) The application of STEM and *in situ* controlled dehydration to bacterial systems using ESEM. *Scanning* **34**: 237–246.
- Wang Y, Lee SM & Dykes GA (2013) Potential mechanisms for the effects of tea extracts on the attachment, biofilm formation and cell size of *Streptococcus mutans*. *Biofouling* **29**: 307–318.
- Weimer PJ, Price NP, Kroukamp O, Joubert LM, Wolfaardt GM & Van Zyl WH (2006) Studies of the extracellular glycocalyx of the anaerobic cellulolytic bacterium *Ruminococcus albus* 7. *Appl Environ Microbiol* **72**: 7559–7566.
- Whitnack E, Bisno AL & Beachey EH (1981) Hyaluronate capsule prevents attachment of group A streptococci to mouse peritoneal macrophages. *Infect Immun* **31**: 985–991.
- Xiao J, Klein MI, Falsetta ML *et al.* (2012) The exopolysaccharide matrix modulates the interaction between 3D architecture and virulence of a mixed-species oral biofilm. *PLoS Pathog* **8**: e1002623.
- Xue X, Sztajer H, Buddrhuhs N, Petersen J, Rohde M, Talay SR & Wagner-Dobler I (2011) Lack of the delta subunit of RNA polymerase increases virulence related traits of *Streptococcus mutans*. *PLoS One* **6**: e20075.